Chapter Three

Application of Laser scanner

Chapter Three

Application of Laser scanner

3-1 Introduction

Turning next to laser ranging, profiling, and scanning, which are the main subjects of the present volume, lasers started to be used by surveyors for distance or range measurements in the mid- to late-1960s. These measurements were made using instruments that were based either on phase comparison methods or on pulse echo techniques. The latter included the powerful solid-state laser rangers that were used for military ranging applications such as gunnery and tracking. On the field surveying side, from the 1970s onwards, lasers started to replace the tungsten or mercury vapor lamps that had been used in early types of EDM (electronic distance measuring) instruments. Initially these laser-based EDM instruments were mainly used as stand-alone devices measuring the distances required for control surveys or geodetic networks using trilateration or traversing methods. The angles required for these operations were measured separately using theodolites. [10]

Later, these two types of instruments were merged with the laser-based ranging technology being incorporated into total stations, which were also capable of making precise angular measurements using opto-electronic encoders. These total stations allowed topographic surveys to be undertaken by surveyors with field survey assistants setting up pole-mounted reflectors at the successive positions required for the construction of the topographic map or terrain model. This type of operation is often referred to aselectronic tacheometry. With the development of very small and powerful (yet eye-safe) lasers, reflectorless distance measurements then became possible. These allowed manually operated ground-based profiling devices based on laser rangers to be developed, initially for use in quarries and open-cast pits and in tunnels (Petrie, 1990). [2]

Given all this prior development of lasers for numerous different field surveying applications, it was a natural and logical development for scanning mechanisms to be added to these laser rangers and profilers. This has culminated in the development of the present series of terrestrial laser scanners that are now being used widely for topographic mapping applications, either from stationary positions when mounted on tripods or in a mobile mode when mounted on vehicular platforms. [10]

3-2 Terrestrial Laser Scanning in Bridge Inspection

Heavy traffic and aggressive environmental conditions can cause unexpected bridge deterioration. Traditional condition evaluation is expensive. An alternative is Terrestrial laser scanning (TLS) which is a non-contact approach that safe, fast, and applicable to a range of weather conditions. This paper reviews applications of TLS on bridge measurement involving geometric documentation, surface defect determination, and corrosion evaluation, and crack identification. Currently, most post-processing of TLS is manual or within third party software. [16]

3-2-1 Principal of Terrestrial laser Scanner

TLS uses either ranging or triangulation scanners. With ranging, the distance between the transmitter and reflecting surface is computed either as the time of travel between signal transmission and reception called the time of flight (ToF) of a laser pulse or the phase difference between the transmitted and received wave, which is referred to as the phase comparison method. The latter one uses a transmitting device and a charge-coupled device sensor to detect the laser spot on an object. Then the three dimensional (3D) position of the reflecting surface element can be derived from the resulting triangle. For bridges and other large structures, ToF scanners are preferred because of their longer range. [15]

The ToF scanner generates scanned points through a series of range measurements with uniform angular increments in both horizontal and vertical planes. This is controlled by rotating and nodding mirrors and rotating head mechanisms. Thus, each sampled point is defined by spherical coordinates with the range measurement, R, horizontal direction, θ, and vertical angle,. α.[15]

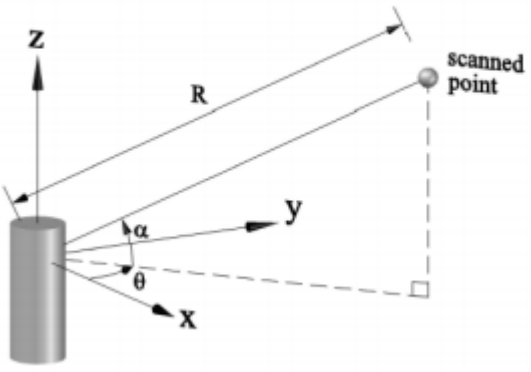

Figure (3-1): The principal of laser beam scanning [4]

A range measurement is the distance from the transmitter to a reflecting surface, R, as expressed in Equation (3.1): [14]

$$R = CT\frac{1}{2} \quad (3.1)$$

where t is the time interval between the emission and the pulse and its reception of the backscattered portion, and c is the velocity of light through air (3x10^8 m/s). A scanner's accuracy is largely based on the accuracy of the time measurement of the electronics integrated into the circuit (Equation 3.1). Furthermore, the ranging accuracy is inversely proportional to the ratio of signal to noise, which depends on various factors such as the power of the received signal, input bandwidth, background radiation, and amplifier noise. [14]

$$\Delta = \frac{1}{2}c\Delta t \quad (3.2)$$

Each raw scanned point (R, θ, α) is automatically converted into a set of three-dimensional Cartesian coordinates (x, y, z) by the scanner software, where the origin coordinate is at the scanner. Beyond the 3D coordinates of the scanned points, the scanner also acquires intensity values, which is a measure of the electronic signal strength obtained by converting and amplifying the backscattered optical power. Pfeifer et al. proposed the relationship between the emitted power, PE and the received power. PR as expressed in Equation (3.3) when the temporal variations of the pulse power are neglected. [14]

$$PR = PE\frac{\cos\alpha}{4R2}\pi\rho\,\eta_{Atm}\eta_{\mathrm{Sys}} \quad (3.3)$$

where ρ is the reflectance of material, R is the range measurement, and ηAtm and ηSys are respectively the atmospheric and system losses. Equation 3 implies that the intensity values strongly depend on the reflectance of the material, the incidence angle underlying a constant of atmosphere, and the range measurement. [14]

By integrating a camera within the scanner, photographs of the scene can be taken simultaneously. From these images red, green, and blue (RGB) values can then be mapped onto each positional data point. Thus, information with each point cloud provided by TLS involves 3D coordinates, intensity values, and RGB values. To understand the capabilities of TLS in surveying bridge structures for inspection, the next section investigates recent work on TLS data processing in that field. [14]

3-1-3 Bridge Inspection

TLS acquires 3D geometric data of a structure's surfaces as discrete data points. That information can be used to either reconstruct 3D models of the structures or to detect surface changes over time. [1]

3-1-3-1 Geometric reconstructions

Some of the earliest applications of TLS to bridges have been for the acquisition of historical arch bridges geometries. In some cases, the surfaces were then derived by mesh triangulation to generate solid models and create a permanent record. In some instances, such as the work by Riveiro et al TLS was combined with close range photogrammetry. Similarly, Lubowiecka et al. combined TLS with ground penetrating radar for a medieval bridge models to provide insight into the internal structure (fill material, arch stones and air water interface) of the bridge. Typically, these efforts rely on third party software or researcher driven algorithms such as that by Armesto et al. who proposed fitting a non-parametric regression method based on a local bivariate kernel smoothing approach from the point clouds for Spain's Segura Roma bridge. [1]

3-1-3-2 Vertical bridge displacement

The first published vertical deflection measurements for bridges was done by Lichti et al. in 2002, who measured displacements of stringers of a wood bridge in Perth, Australia. Vertical displacements were estimated by comparing fitting lines of the bottom and top of each stringer cross-section under loaded and unloaded conditions. Results showed that stringers deflections based on TLS data were larger than ones from image-based methods. [1]

Subsequently, Zogg and Ingensand monitored deformations of the Felsenau bridge subjected to a static load of 54 tons performed at several sections of the viaduct. Third party software was used to determine vertical displacements by comparing the 3D point cloud from the unloaded condition against the loaded condition. The TLS-based results were no more 3.5mm larger than ones based on precision levelling. [1]

When measuring deflections of the Pentele bridge under the static load, Lovas et al reported that vertical displacements from TLS data gave strong correlations with traditional methods, although it over predicted the high-precision levelling and under predicted the total stations. [1]

Paffenholz et al. proposed a cell-based method to estimate vertical displacements. The scanned region was divided into sub-areas of 0,25m x 0,25m, and the median of z coordinates of each sub-area was used to determine the vertical displacements. Deflections up to 3mm were reported, but the accuracy was not. Finally, Berenyi et al. noted that TLS can be used to measure the movements of the pylons and cables, whereas the traditional method cannot be done or unaffordable. [1]

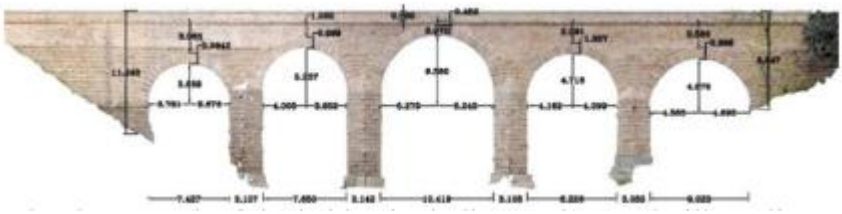

a) Orthophotograph of the bridge including arches and pillars dimensions

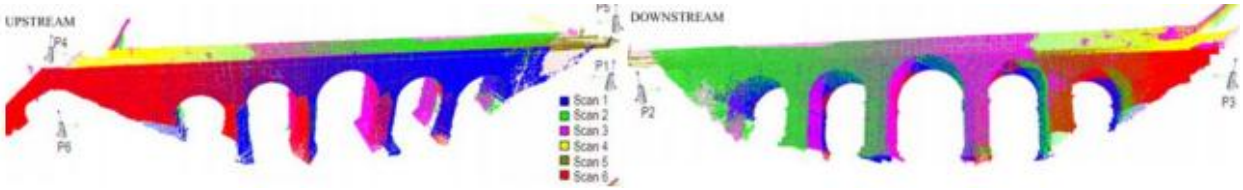

b) Scan stations and point clouds of the bridge

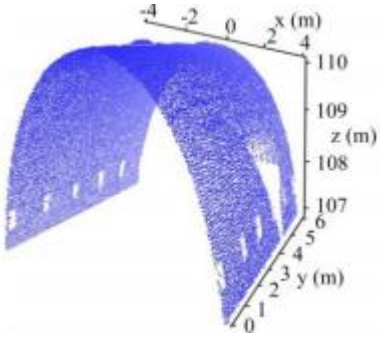

c) Point cloud of the second arch of the bridge

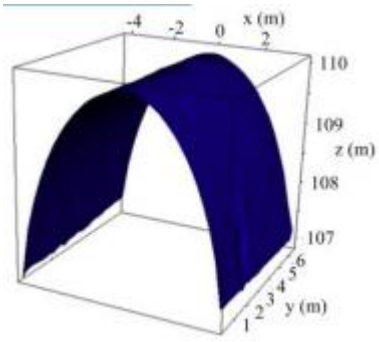

d) 3D arch model obtained for the bandwidth of 0,06 used in the kernel estimation

Figure (3-2): Reconstructing bridge models from TLS data by a non-parametric estimation algorithm [1]

3-3 Cultural Heritage Applications

Cultural heritage is a testimony of past human activity and, as such, cultural heritage objects exhibit great variety in their nature, size and complexity, from small artefacts and museum items to cultural landscapes, from historic buildings and ancient monuments to city centers and archaeological sites. Due to the rapidity of data capture and the ability to obtain point clouds instantaneously, laser scanning has become an essential tool along with image-based documentation methods. Total station surveys, on the other hand, require more time on site and usually do not deliver the same level of surface detail. [3]

Cultural heritage objects and sites are often a conglomerate of irregular surface geometries. Although photogrammetry will work for similar structures, laser scanning provides dense 3D information in almost real time with a high capacity for visualization as a first on-site preresult. Laser scanning is of interest where documentation is usually a complex task. The variety of applications includes pure visualisation as well as heritage recording and as-built documentation. [3]

3-3-1 Accurate site recording: 3D reconstruction of the treasury (Al-Kasneh) in Petra, Jordan

The ancient Nabataean city of Petra has often been called the eighth wonder of the ancient world. Petra city in south-western Jordan (Figure 8.1) prospered as the capital of the Nabataean empire from BC 400 to AD 106. [9]

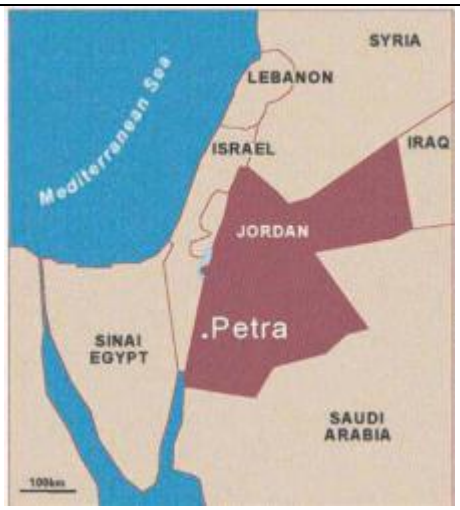

Figure (3-3): Geographical situation of Petra, Jordan [9]

Petra's temples, tombs, theatres and other buildings are scattered over 400 square miles, carved into rose-coloured sandstone cliffs. When a visitor enters Petra via Al-Siq, an impressive two-kilometre crack in the mountain, he will first see Al-Khasneh, which is probably the most famous object in Petra. The Al-Khasneh façade is 40 m high and remarkably well preserved, probably because the confined space in which it was built has protected it from the effects of erosion. The name Al-Khasneh means "treasury or tax house for passing camel caravans", but others have proposed that the Al-Khasneh monument was a tomb. Behind the impressive façade there are large square rooms that have been carved into the rock. [3]

The 3D laser scanning system Mensi GS100 was applied. The scanner features a field of view of 360o in the horizontal direction and 60o in the vertical direction, enabling the collection of full panoramic views. The distance measurement is obtained using the time-of-flight measurement principle based on a green laser at 532 nm allowing an object distance between 2 and 100 m. The system is able to measure 5000 points per second. During data collection a calibrated video snapshot of 768 s 576 pixel resolution is additionally captured, which is automatically mapped to the corresponding point measurements. Because of the complex structured sites, multiple scanner stations had to be chosen to avoid most of the occlusions. [9]

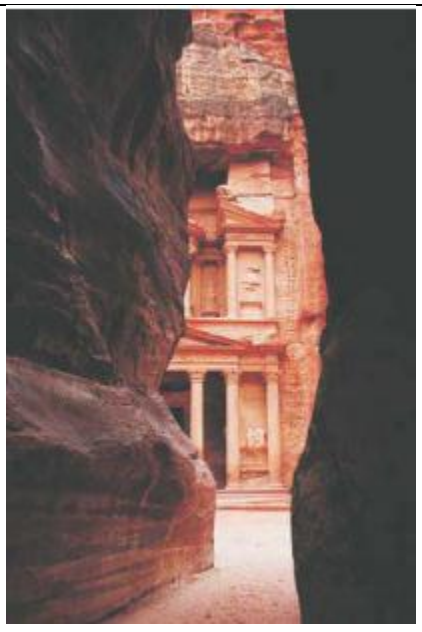

Figure(3-4): The Outer Siq at the Khasneh al-Faroun [6]

For texturing of the 3D model, additional images were collected by a Fuji S1 Pro camera, with a focal length of 20 mm and a sensor format of 1536 s 2034 pixels. [6]

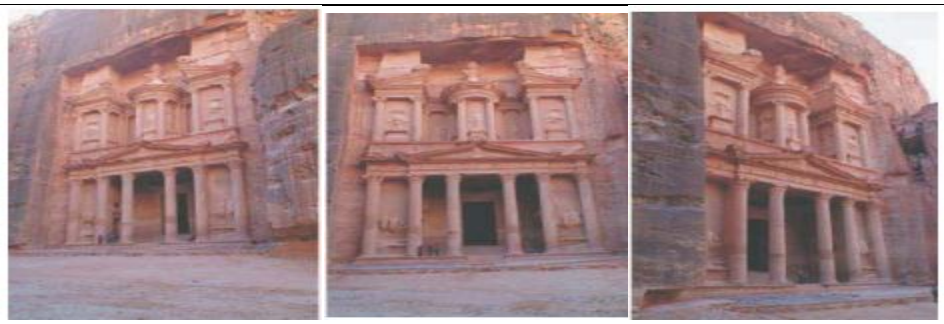

Figure (3-5): Images collected using a Fuji [9]

The acquired 3D point clouds have been processed using Innovmetric's PolyWorks™ Software. Registration of the scans for both models was done using corresponding points. The models produced have an average point spacing of 5 cm with more than 2 000 000 triangles for the entire model. [6]

Figure (3-6): 3D model of Al-Khasneh [6]

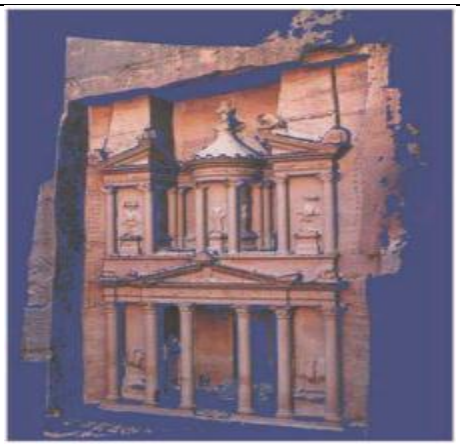

Figure (3-7): Final textured model using four images [6]

The work was carried out by Yahya Alshawabkeh and Norbert Haala, Institute for Photogrammetry (IFP), University of Stuttgart, Germany, with support from Hashemite University of Jordan, Petra, Regional Authority and Jerash Municipality ,Jordan. [11]

Performing projective texture mapping to generate photo-realistic models of the complex shaped objects with minimal effort, it was necessary to compute visibility information to map the image only onto the portions of the scene that are visible from its camera viewpoint. For this purpose an efficient algorithm addressing image fusion and visibility has been developed . [9]

The result was a textured 3D model of the site (Figure 8.5) demonstrating the possibilities of the integration of laser scanning and photogrammetry for data capture of historic scenes. [6]

3-3-2 Archaeological site: scanning the pyramids at Giza, Egypt

In 2004 was to apply Scanning of the Pyramids and test the latest state-of-the-art terrestrial laser scanners combined with a calibrated digital Final textured model using four images camera for high-accuracy, high-resolution and long-distance topographic scanning in archaeology. [7]

A long-range laser scanner Riegl LMS Z420i combined with a calibrated Nikon D100 digital camera was used for this project. The combined sensor of a high-performance long-range laser scanner and a calibrated and orientated high resolution digital camera provides scan and image data.. [6]

The three main objectives of the Scanning of the Pyramids project are:

1- The collection of high-resolution and high-accuracy topographic data for the creation of a digital elevation model of the Giza plateau.
2- 2-A 3D documentation of the Cheops Pyramid and surroundings.
3- 3-A 3D documentation of the Sphinx.
4- The Riegl Z420i scanner was taken to the top of the Great Pyramid of Cheops for a full ten hours of data collection. [14]

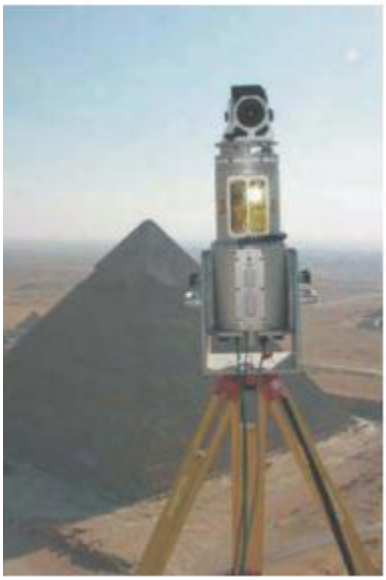

Figure (3-8): LMS-Z420i with calibrated high-resolution digital camera Nikon D100 at the top of the Cheops Pyramid, Egypt [14]

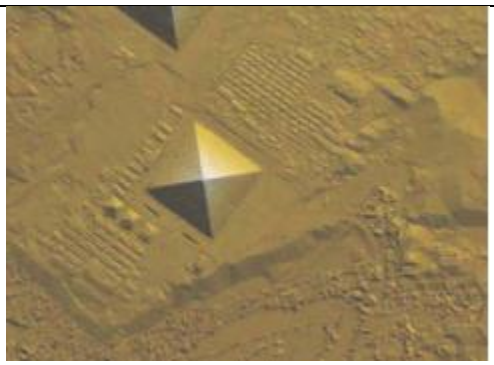

Figure (3-9): Overview and detail of the digital elevation model of the Giza Plateau created using four single scans from the top of the Cheops Pyramid visualized in ARC GIS 8.2.[14]

Figure (3-10): Single scan from the north and east faces of the Chephren Pyramid visualised as a coloured point cloud.[14]

Figure (3-11): Triangulated point cloud of the Sphinx textured in Rican Pro, combined from seven scanner positions: six from the ground and one from the Cheops Pyramid.[14]

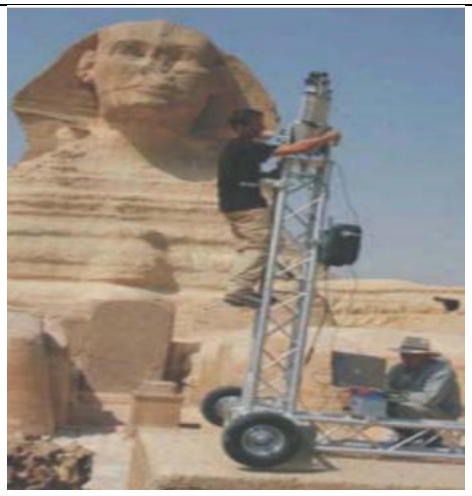

Figure (3-12): Mobile scanner in front of the Sphinx[14]

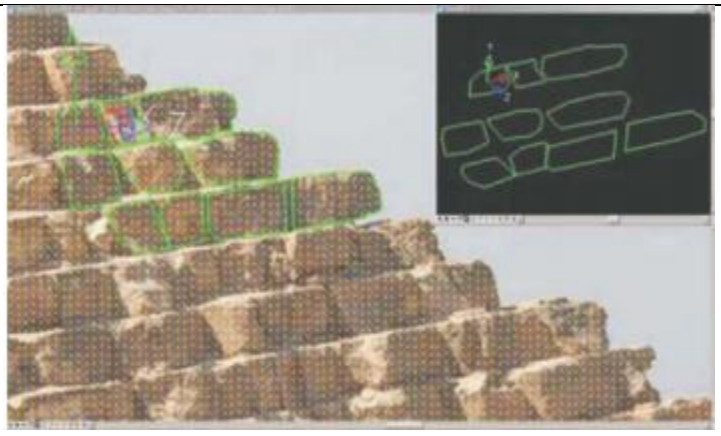

Figure (3-13): Single stones can be directly drawn in global 3D coordinates and made visible in the point cloud, superimposed with a photograph using the Micro station application PHIDIAS.[14]

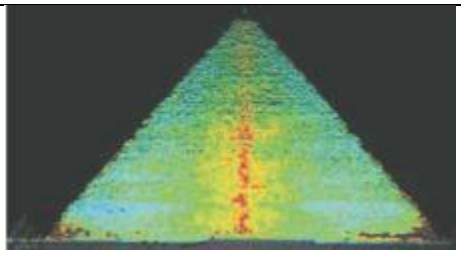

Figure (3-14): Anomalies of the Cheops Pyramid: horizontal projection of the west side with color-coded deviation from the plane.[14]

These data have been processed automatically with human interaction in some processing steps for the generation of textured triangulated surfaces (Figure 3.10) and orthophotos with depth information (Figure 3.14).

3-3-3 The archaeological project at the Abbeynof Niedermunster, France

Located at the bottom of Mount Sainte-Odile, the Abbey of Niedermunster, Alsace, France can be considered as the origin of the sanctuary. Built between AD 1150 and 1180, the Roman-style Abbey was devastated during the War of the Peasants (1525) and by two fires, in 1542 and 1572. The site was then used as a quarry until the nineteenth century. The great western massif of the basilica, still in elevation, and the relics of the crypt allow the beauty of the original buildings to be imaged. [2]

During the first stage, the archive archaeological records were georeferenced in a Geographical Information System after an accurate topographic survey. The second stage of scanning was accomplished in two steps: scanning of the abbey's area in its current state, followed by supplementary scanning site details. [2]

Data acquisition consisted of scanning the complete site using 3D terrestrial laser scanning [Koehl and Grussenmeyer, 2008]. A Trimble GX Advanced scanner was used.This allowed the acquisition of point clouds for which the density was defined by the operator according to the expected degree of detail. A grid density of 1000 points/m2 was generally used. The obtained point clouds were georeferenced; the information for every point was thus constituted by *X*-, *Y* - and *Z*-coordinates in the ground coordinate system, completed by intensity or colour. For the complete digitising of the site, about 15 scanner positions were used, which resulted in 40 different scans, giving a total of approximately 30 million points (Figure 3.15). [2]

Figure 3.16 is an illustration of the point cloud of the occidental block which is still standing up to its first level. Interior parts such as stairways and the porch have also been scanned. Eight scanning stations were used for this part of the project. Figure 3.17 illustrates the process of combination of meshed surfaces computer from the terrestrial laser scanning point clouds and a CAD model used in the case of flat surfaces. The fusion of the two models was used for the creation of the complex and ruined parts of the project. For the constitution of the 3D model, textures were mapped as shown in Figure3.18. Some parts have been textured, others were only face-coloured. The inner parts are shown by application of surface transparency. [14]

Figure (3-15): Fusion of point clouds in one project. [14]

Figure (3-16): Fusion of point clouds of the occidental block.[14]

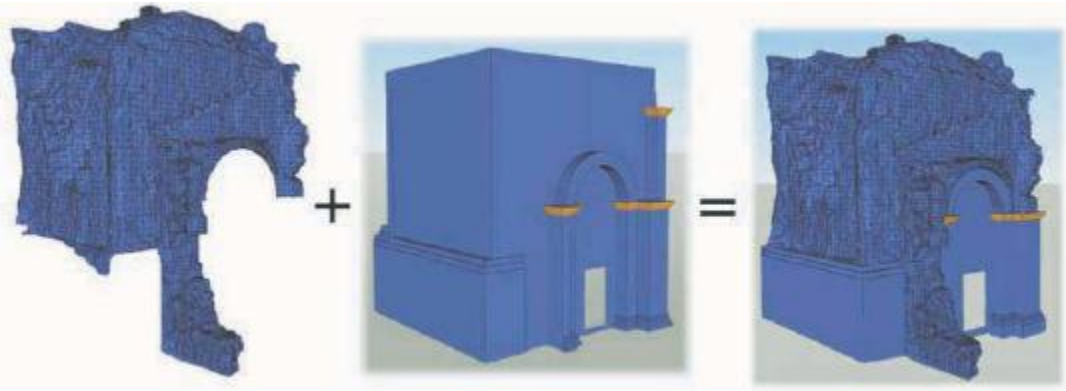

Figure (3-17): Model creation as CAD extrusions and meshed model from point clouds. [14]

Figure (3-18): Textured model of the occidental block.[14]

Figure (3-19) shows a detailed point cloud of the crypt. This part of the project is composed of two stairways, some pieces of pillar and an inner vaulted wall. As in the other parts of the abbey, the walls remained in a good state of conservation, but other parts were ruined. The resulting model (Figure 3-20) combines meshed point clouds and CAD models. The structure lines of the main parts used in the modeling process result from a manual segmentation. Figure. (3-21) is the result of the texturing process of the crypt model. [2]

Figure (3-22) illustrates the different representation modes in the case of the acquisition of a pillar base. Terrestrial laser scanning offers the possibility of viewing the different point clouds in a colour mode. This is used to show the different segmented clouds. Intensities were also acquired by the laser scanner. The intensity mode can be used to analyse the responses of the scanner according to the surface texture. The true colour rendering mode uses the colour of each point according to its position in an image acquired by the laser scanner camera. The last illustration shows the CAD. [2]

Figure (3-19): Point cloud of the crypt. [14]

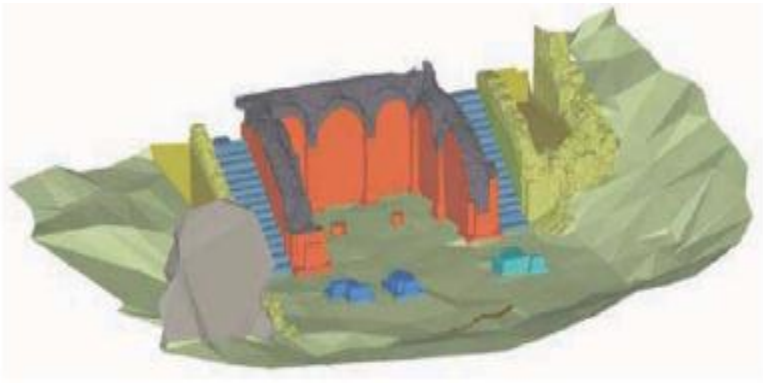

Figure (3-20): CAD model from terrestrial laser scanning data.[14]

Figure (3-21): Textured model of the crypt.[14]

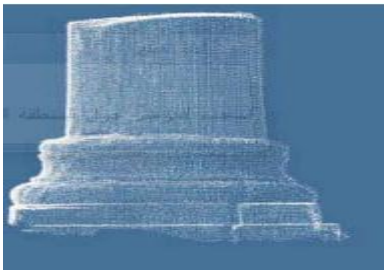

(a) white point cloud

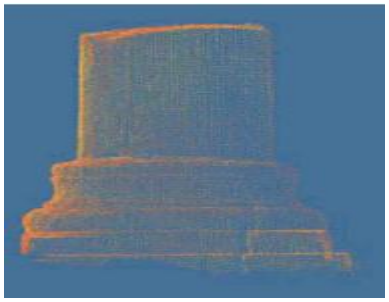

(b) intensity cloud

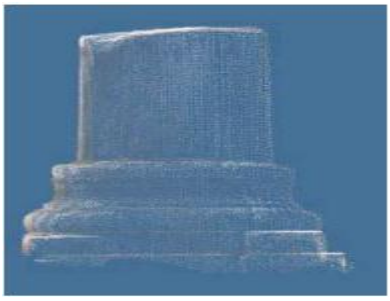

(c) true colour

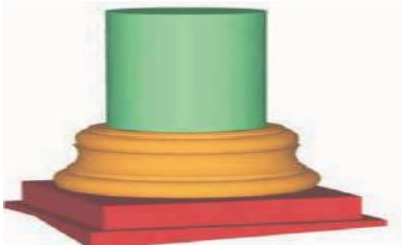

(d) CAD model.

Figure (3-22): Detail of a pillar [14]

Figure (3-23): 3D model of the Niedermunster Abbey site.[14]

model extracted from the point clouds using a segmentation of the profile. An extrusion process was then used for design of the model. [2]

Figure (3-23) shows the 3D model of the whole site, allowing animations and walkthroughs. [2]

3-4 Forest inventory applications

Forest inventory is a task which has to be fulfilled by forest authorities at regular time intervals to monitor the state of their forests. It includes the determination of a number of parameters characterizing the forest. As full area coverage is an unrealistic goal in forest inventory using conventional techniques, inventory schemes based on data acquisition in isolated plots and statistical inference methods have been developed. Some of the most important parameters to be determined in forest inventory are the number of trees in a certain plot, the determination of the diameters at breast height and the tree heights. Terrestrial laser scanning, combined with reliable automatic data-processing techniques, may provide an interesting tool to bridge the gap between conventional inventory techniques and airborne laser scanner data-processing schemes and to facilitate data acquisition for 3D individual tree geometry parameters in large plot. [6]

The data-processing chain used in the studies can be outlined as follows:
1- Digital terrain model reduction: the digital terrain model is determined by a simple height histogram analysis searching for minima in predefined XY meshes of the laser scanner data, followed by a neighborhood consistency check and bilinear interpolation in the meshes. All laser scanner points are reduced to this terrain model. [7]

2- Segmentation and counting of trees: the tree detection process is based on mathematical morphology techniques, extended from raster image analysis to irregularly distributed points in horizontal slices of the laser scanner data. [7]

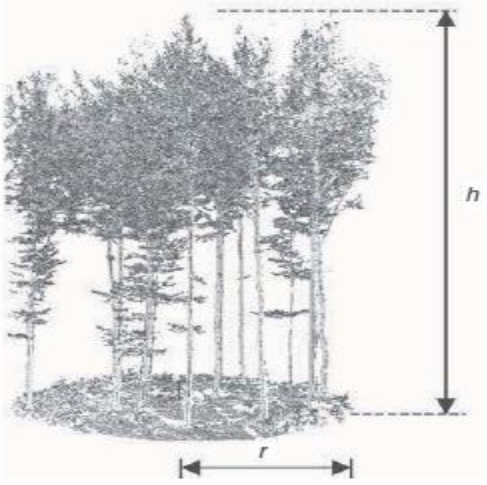

Figure (3-24): point cloud of a single panoramic scan [5]

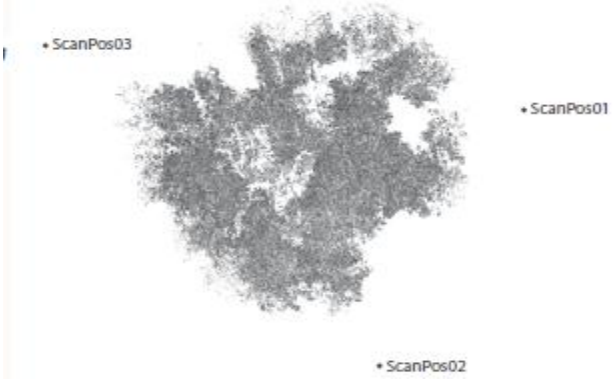

Figure (3-25): point cloud from a multiple scan mode with three instrument position [5]

3- Determination of diameter at breast height: the diameter at breast height (DBH) is defined as the diameter 1.3 m above the finished grade at the end of the trunk.It is determined by fitting a circle into the point cloud of each detected tree and analyzing the results using robust estimation techniques. [7]

4- Tree height determination: the tree height is calculated as the height difference between the highest point of the point cloud of a tree and the representative ground point using a similar procedure to that reported.Generally, tree height determination procedures remain rather vague due to under sampling, occlusions and wind effects in the crown. [7]

5- Stem profiles: repeating the technique of stem position and diameter at breast height determination in predefined height intervals at the same (X,Y)-location, stem profiles containing information on shape, uprightness and straightness can be determined. The probability of gross errors in the diameter determination is further reduced by using knowledge of the tapering of the stem in a subsequent filtering operation. [7]

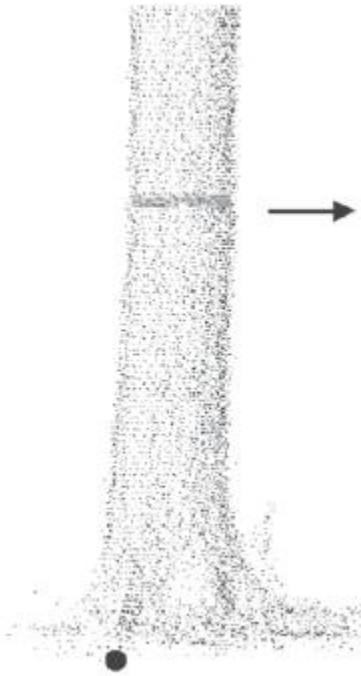

Figure (3-26): Ground point of a tree on sloping terrain [6]

Of tree detection was 97.5%. Type I errors (trees which were not detected) were mostly caused by full or partial occlusions of stems in single panoramic scan data. Type II errors (false detections) could largely be eliminated in later processing steps by checking the tree height or by an analysis of the stem profile. From a comparison with conventional calliper measurements, an RMS error of 1.8 cm could be obtained for the automatic determination of diameter at breast height. This value contains the laser scanner instrument precision as well as the precision of caliper measurement and deviations of the stem from circularity. Automatic tree height determination turned out to be much more critical: compared to hand held tachymeter height measurements, an RMS error of 2.07 m was obtained. This error has to be attributed to both occlusions in the point cloud and the limited precision of the reference measurements. Vertical stem profiles were derived by applying the circle fit procedure at multiple height steps. A comparison with harvester data yielded an RMS profile diameter difference of 4.7 cm over the whole tree, with larger deviations occurring in the lower and upper part of the stem. Over the economically most relevant branch and root free part of the stem, the RMS diameter deviation was only 1.0 cm. [6]